Formation of a cylindrical dust void in a plasma crystal due to a potential bump

Yu Zhang,* Xiaogang Wang, and Jinyuan Liu
State Key Laboratory of Materials Modification by Laser, Ion and Electron Beams, Dalian University of Technology, Dalian 116024, China

(Received 7 April 2008; published 25 July 2008)

Formation of a cylindrical dust void in dust plasma crystals is simulated using the molecular dynamics method in a three-dimensional fluid sheath model with axisymmetry. The dust trajectories are integrated under a self-consistent field composed of the interactions with the electrostatic sheath field, gravity, drags, wakes, and nonlinear screened Coulomb forces. The simulation successfully explains how a uniform dust cloud transforms into a dust void as the dust particles grow to a sufficient size [D. Samsonov *et al.*, Phys. Rev. E **59**, 1047 (1999)] or the power supply and/or gas pressure increases to certain levels [R. P. Dahiya *et al.*, Phys. Rev. Lett. **89**, 125001 (2002)]. It is found that instead of the ion drag or thermophoretic force effect, the formation of the dust void in the axisymmetric three-dimensional sheath is due to a gentle potential bump in the central region of the electrode caused by the cylindrical geometry.

DOI: 10.1103/PhysRevE.78.016405 PACS number(s): 52.27.Lw, 52.40.Kh

I. INTRODUCTION

Complex plasmas, with many analogies to other strongly coupled systems in different fields of scientific research and the great advantage of visibility, have been among the most extensively studied areas in recent decades. Voids formed in such complex plasmas have been observed under various environments, such as in research labs, industrial plasma-processing devices, and microgravity experiments in spacecraft [1–7]. In certain cases, the void was induced by an externally introduced negative potential [2,8]. In general, however, the voids developed spontaneously, due to strongly nonlinear instabilities, to form typically a small and stationary region surrounded by a sharp boundary, completely free of dust particles. It was found in laboratory experiments that the size of the dust particles, the supply power, and the neutral gas pressure were crucial parameters for void formation [1,6,7]. In other words, the voids emerged from a uniform dust cloud as the dust particles grew to a sufficient size [1] or the power supply and/or gas pressure increased to certain levels [6,7].

To explain the void formation process, various mechanisms have been proposed, such as the thermophoretic force due to the temperature gradient and finite dust size [4], the ion drag on dust particles [1,9,10], or ionization instabilities in the presence of ion drag and neutral-particle collisions [11–15], as well as a model of force balance between the repulsive screened Coulomb interaction and a van der Waals–like cohesive force [6]. However, all these theories were in either one- or two-dimensional geometries with axisymmetry; a self-consistent model with vertical distribution of the sheath electrical field is lacking.

To systematically investigate the evolution and dynamics of dust voids suspended in a plasma sheath, in this paper we develop a three-dimensional (3D) molecular dynamics (MD) model for dust particles in a plasma sheath caused by a pan-shaped electrode. The formation of dusty crystalline structures and the void is simulated in a 3D cylindrical sheath with its confining potential in certain ways qualitatively agreeing with the experimental parameters of Paeva *et al.* [6,7]. We then demonstrate that the dust void forms as the size of the dust particles, the plasma density, or the biased voltage is changed in a similar way as in the experiments [1,6,7], e.g., the crystal transforms into a void structure as the particle size grows, or the plasma density increases, or the biased voltage gets higher. We further show that, in the void formation process, neither the thermophoretic force nor the ion drag force is significant in the void region. The only force balancing the repulsive screened Coulomb force to maintain a sharp dust density jump on the void edge is an electrostatic force generated by a gentle potential bump in the central sheath region. A brief discussion of the phenomenon then concludes this work.

II. SHEATH AND DUST EQUATIONS

Crystalline structures in complex plasmas have been observed in many laboratories [16–19]. In such organized structures, the dust particles, usually with a large negative charge due to the high mobility of electrons, are trapped in a plasma sheath and subject to a screened Coulomb interaction. In general, a concave or pan-shaped electrode is applied to provide a horizontal confinement. Such a sheath can be simulated by a fluid model in a 3D cylindrical geometry. Using the parameters in Refs. [6,7], a sketch of the sheath is shown in Fig. 1 where $r=R_0$ and $z=Z_0$ are the boundaries of the simulation box and $z=0$ $(r<r_0)$ and $z=z_0$ $(r>r_0)$ the electrode.

In the fluid sheath model, we assume that electrons are Boltzmannian, $n_e=n_0\exp(eV/T_e)$ and the streaming ions are described by continuity $\vec{\nabla}\cdot(n_i\vec{u}_i)=0$ and force balance $m_i(\vec{u}_i\cdot\vec{\nabla})\vec{u}_i=-e\vec{\nabla}V(r,z)-\vec{\nabla}P$, where the pressure $P=n_eT_e+n_iT_i$, n_e and n_i are the electron and ion densities, T_e and T_i are their temperatures, n_0 is the plasma density at the upper boundary $z=Z_0$, e is the elementary charge, m_i is the ion mass, V is the sheath potential, and $\vec{u}_i$ is the ion streaming

*yuzhang@stuednt.dlut.edu.cn

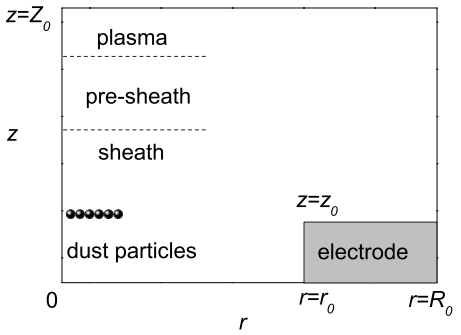

FIG. 1. Sketch map of the simulated sheath.

velocity. The model is then closed with the Poisson equation $\nabla^2 V=-4\pi e(n_i-n_e)$.

Instead of taking the plasma-sheath interface as the upper boundary, to consider the cylindrical effect of the pan-shaped electrode, the fluid equations are solved in the full scale from the electrode to the plasma region, including the plasma, presheath, and sheath regions [20]. The upper boundary $z=Z_0$ then is so deep into the plasma region that the cylindrical effect of the electrode shape is totally screened at the boundary. The appropriate boundary conditions are then as follows. At the upper boundary $z=Z_0$, the plasma conditions are taken as $u_i=0$ and the potential V=0 from the quasineutrality $n_e=n_i=n_0$. At the electrode $z=0$ $(r<r_0)$ and $z=z_0$ $(r>r_0$, the potential is $V=V_0$ with V_0 the electrode bias voltage. At the radial boundaries, we can assume that R_0 is large enough to make the boundary condition $\partial/\partial r=0$; and at $r=0$, $\partial/\partial r=0$ and $u_{ir}=u_{i\theta}=0$ due to the axisymmetry.

For the dust particles then, a MD method is applied. The particles are immersed in the plasma sheath subject to interactions with the electrostatic sheath field, gravity, drags, wakes, and screened Coulomb forces. Their trajectories are then integrated under a self-consistent field composed of these interactions. The equation describing the motion of the jth dust particle can be written as

$$M\frac{d\vec{U}_j}{dt}=-Q_j\left(\vec{\nabla}V+\sum_{j\neq k}[\vec{\nabla}\phi_{k,\mathrm{wake}}+\vec{\nabla}\phi_{Dk}(\vec{R}_{jk})]\right)+m_i n_i\gamma_{id}\vec{u}_i-m_i n_n\gamma_{nd}\vec{U}_j, \quad (1)$$

where M, $\vec{U}$, and Q_j are the mass, velocity, and charge of the jth dust particle, $\phi_{k,\mathrm{wake}}$ the wake potential created by the kth particle, $\phi_{Dk}(R)$ the nonlinear screening Coulomb potential of the kth particle, with γ_{id} and γ_{nd} the ion drag frequency and the neutral collision frequency, $R_{jk}=\vec{R}_j-\vec{R}_k$ the distance between the jth and kth particles, and $\vec{g}$ the gravity accelerator. The ion drag can be written as $\gamma_{id}=n_i\sigma_i d(u_i)u_i$ [23]. The dust charge is calculated by the orbit-limited model including the effect of the neutral particle charge exchange collisions [24]. The wake potential and the nonlinear screening Coulomb potential are computed by the model developed in Refs. [25,21], respectively. In the simulation, the size and shape of the electrode in the model are selected to be the same as in the experiment of Dahiya *et al.* [6], with a 3.0 cm diameter and 0.3 cm depth cylindrical well. In the simulation, a certain amount of identical dust particles is injected into the sheath region randomly and then moved subject to the forces on the right-hand side of Eq. (1) self-consistently until a steady state is reached due to the high neutral gas dumping. A crystal can thus be formed.

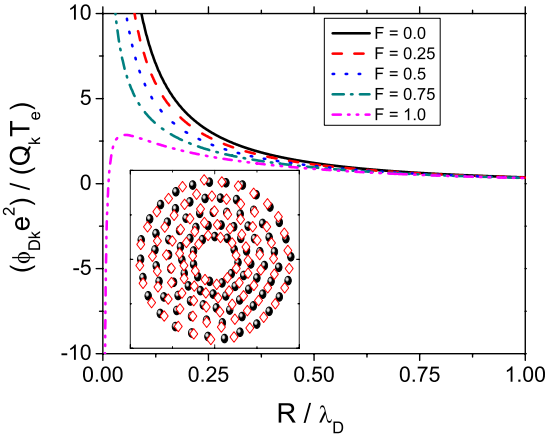

FIG. 2. (Color online) Nonlinear screening Coulomb potential with different F and comparison of void structure between (solid circles) nonlinear screening Coulomb potential and (open diamonds) Debye-Yukawa potential when $T_i=0.1$ eV, $T_e=2.0$ eV, $n_0=2\times10^8$ cm^{-3}, $V_0=-100$ V, and $r_d=2.0$ μm.

III. RESULTS AND DISCUSSION

The influence of nonlinear screening effects and the dynamic screening effect on void structures are discussed first. The nonlinear screening Coulomb potential can be rewritten as

$$\phi_{Dk}(R)=[Q_k\exp(-R/\lambda_D)]/R\{1+F[\exp(R/\lambda_D)E_i(-3R/\lambda_D)+E_i(-R/\lambda_D)]\},$$

where λ_D and $F=(eQ_k)/(4\lambda_D T_e)$ are the Debye length and a nondimensional parameter, respectively; $E_i(-r)=-\int_r^\infty dy\exp(-y)/y$ is the exponential integral function [22]. Only when $F\geqslant 0.5$ is the nonlinear screening Coulomb potential significantly different from the Debye-Yukawa potential as shown in Fig. 2. For the present case, the largest F of all the dust particles is 0.0405. As a result, simulation with the Debye-Yukawa potential will not induce much error, as shown in Fig. 2. However, the nonlinear screening effect will be significant for the dust particles with larger charges. The dynamic screening effect can also be considered in the simulation by modifying the term $\exp(R/\lambda_D)$ with $\exp\{-R/[\lambda_D(1+U_k^2/v^2)^{1/2}]\}$, where $v=(T_e/m_e)^{1/2}$ is the electron thermal velocity [26]. The value U_k^2/v^2 is a small value due to the huge mass difference between dust particles and electrons, especially for a static state dust crystal structure, $U_k\sim 0$. The dynamic screen effect is neglected to simplify the simulation.

In comparison with the experiments, we then vary the size of the dust particles, the plasma density, and/or the bias voltage of the electrode sheath to form the void. In Ref. [1], a void was developed in an initially almost uniform dust crys-

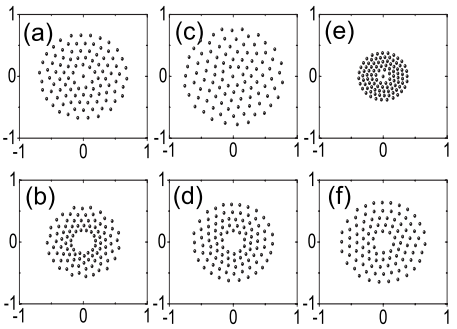

FIG. 3. The structure of crystal of silicon dust particles in the sheath with T_i=0.1 eV and T_e=2.0 eV, as well as for (i) n_0=2 $\times 10^8$ cm^{-3}, V_0=−100 V: (a) r_d=1.0 μm, (b) r_d=4.0 μm (ii) n_0 =2$\times 10^8$ cm^{-3}, r_d=2.0 μm: (c) V_0=−20 V, (d) V_0=−100 V (iii) V_0=−100 V, r_d=1.5 μm: (e) n_0=5$\times 10^6$ cm^{-3}, (f) n_0=2 $\times 10^8$ cm^{-3}.

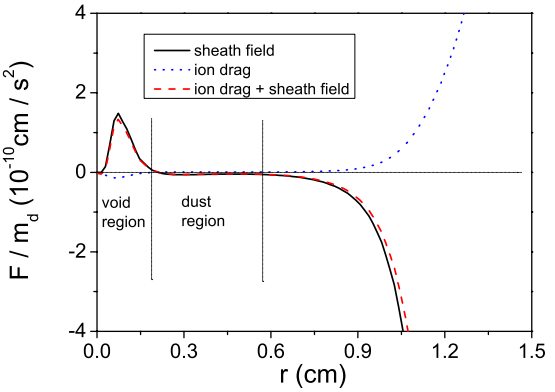

FIG. 4. (Color online) Radial forces acting on a test dust particle, scaled by 10^{-10} cm/s^2, as a void forms under the conditions in Fig. 3(b), with the dashed line representing the sheath field force, the dotted line the ion drag force, and the dash-dotted line the sum of the sheath field and the ion drag forces.

talline structure as the dust particles grew to a sufficient size. This phenomenon coincides to the simulation result shown in Figs. 3(a) and 3(b), where in the same plasma circumstances, as the particle size is enlarged from 1.0 to 4.0 μm, a void emerges [Fig. 3(b)] from the crystalline structure [Fig. 3(a)]. In other experiments [6,7], a dust void was grown as the supply power and/or neutral gas pressure increased. In the simulation, as the magnitude of the biased voltage on the electrode increases from 20 to 100 V, the void shown in Fig. 3(d) then forms in the crystal shown in Fig. 3(c). Moreover, the void can be created by changing the plasma density, shown in Figs. 3(e) and 3(f) where a void is found when n_0 jumps about two orders of magnitude. We have to point out that the plasma density is scaled approximately linearly with the input power or the pressure under experimental conditions [27]. Therefore, the density growth is subject to power and/or pressure increase. This is again in agreement with the observations [6,7].

In particular, the simulation results have a surprisingly good agreement with other experimental data in Refs. [6,7], e.g., the dust void diameter and the cloud diameter in the case of Fig. 3(b) are 0.44 and 1.19 cm, very close to the numbers shown in Fig. 1 of Ref. [6], when the same parameters are applied.

To understand the void formation mechanism, various interactions have been suggested, such as the thermophoretic force [4], the ion drag on dust particles [1,9,10], or the force balance between the repulsive screened Coulomb interaction and a van der Waals–like cohesive force [6]. In our calculation, an isothermal sheath is assumed. Therefore, the effect of the thermophoretic force vanishes. Furthermore, on the right side of Eq. (1), no van der Waals–like cohesive force has been taken into account. The only possible candidate left then is the ion drag. To examine if ion drag is the main force responsible for the void formation, we calculate the radial forces other than the dust Coulomb repulsion acting on a test dust particle under the conditions in Fig. 3(b). A test particle with the same size as the others is put on the crystalline layer and moved in the radial direction from the center. It can be clearly seen in Fig. 4 that the ion drag force shown as a dashed line is in fact negative, i.e., pointing to the center in the void region. In the dust region, although it changes to positive, in the direction pushing the dust away from the center, the ion drag force is very small. In fact, we surprisingly find that it is not the ion drag but the radial electrostatic sheath field force, shown as a solid line in Fig. 4, that pushes the dust particles away from the central region to form the void. Such a force indicates a potential barrier in the void region that prevents the dust particles from entering the region. Then it immediately raises two questions: how is the barrier created, and are any such barriers found in other experiments or simulations?

In Fig. 5 where the magnitude of the sheath potential $-V(r)$ for different horizontal levels z is shown, one can find a very gentle potential bump indeed rising in the central region of the sheath to repel the dust particle. Clearer details are demonstrated in Fig. 6, for the relative potential magnitude $-[V(r)-V(0)]$. In fact, in the experiment reported in Refs. [6,7], a similar rise of a central potential was also found and clearly shown in Fig. 4 of Ref. [7]. It is true that no such evidence has been reported numerically. Nevertheless, previous simulation studies were either one dimensional with an infinite dust cloud volume [11], or, for example, in

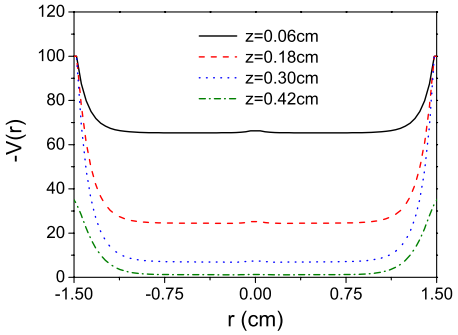

FIG. 5. (Color online) Negative value of sheath potential $-V(r)$ for different horizontal levels, with R_1=1.5 cm, Z_1=0.3 cm, T_i =0.1 eV, T_e=2.0 eV, n_0=2$\times 10^8$ cm^{-3}, and V_0=−100 V; the solid line is at the level z=0.06 cm, the dashed line at z=0.18 cm, the dotted line at z=0.30 cm, and the dash-dotted line at z=0.42 cm.

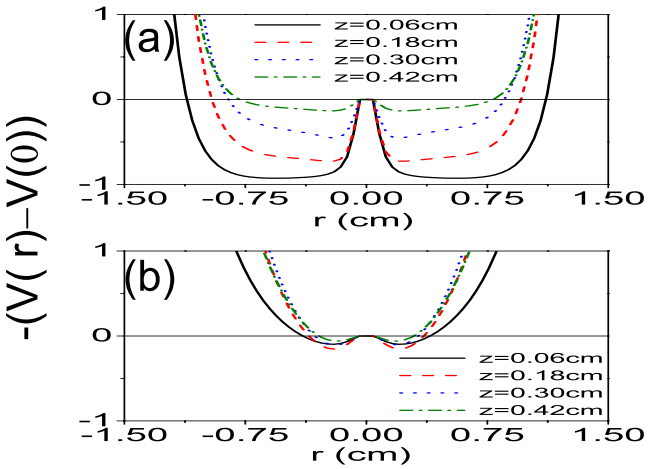

FIG. 6. (Color online) Sheath potential relative to $V(0)$, as $-[V(r)-V(0)]$ for different horizontal levels, with other parameters the same as in Fig. 5, and n_0=(a) 2×10^8 and (b) 5×10^6 cm^{-3}.

an axisymmetric layer with a confinement potential $-Kr^2$ approximately describing a bowl-shaped electrode [28]. In our simulation, however, the electrode is chosen to be the same as in the experiment with a totally flat bottom at $z=0$ and a sharp confinement edge at $r=r_0$ [6,7]. The central potential bump and a potential well for the negatively dust charged particles in between the bump and the confinement edge can be formed in such a geometry.

In Figs. 5 and 6, a few important features of the potential wells are found. (i) It can be demonstrated that in our 3D sheath model the lower the level z the deeper is the potential well. In other words, the effect of the potential bump is much stronger in the lower part of the sheath than in the upper part. It can be seen in the figures that for $z=0.42$ cm the potential in the central region is almost flattened. (ii) On the other hand, for the same height z, shown in Fig. 6, the potential bump is weakened as the plasma density is reduced. Thus, unlike previous models that apply only for certain experiments, the results obtained above can explain most observed phenomena. For example, although the force balance model with the van der Waals–like cohesive force was a good fit for the growth of the void edge, it strongly depended on the assumption that the outer radius of the dust cloud was assumed already to be known as observed [6]. Therefore, the model neither explained why the outer radius of the dust cloud should be as observed, nor offered any clear picture for the void formation process due to the dust size increase. On the other hand, the ion drag might be a reasonable mechanism for the void formation due to the dust size variation. In the 3D geometry, nevertheless, the ions in the central region hardly stream horizontally but stream vertically due to the fact that the horizontal confinement electrode ring $r=r_0$ is many Debye lengths away and therefore almost totally screened. However, from the features shown above in our 3D simulation, it is easy to explain why the void is formed as the dust size, the supply power, and the neutral gas pressure change. If the dust particles are very small, their equilibrium position is in the upper part of the sheath where the potential well effect is extremely weak. Thus there is no void formed. As the dust particles grow to a sufficient size, however, due to the force balance, they fall to a lower level where the central potential bump is big enough to push the particles away from the region. A void then emerges. The process is shown in Figs. 3(a) and 3(b). Also, the void appears from a crystal as the result of a high input power and/or neutral gas pressure. As a result of the power and/or gas pressure increase, the plasma density goes up. For a relatively low density, for example $n_0=5\times10^6$ cm^{-3}, a very shallow central potential well is then established as shown in Fig. 6(b) and the particles confined in the sheath form a crystalline structure [Fig. 3(e)]. For a high density $n_0=2\times10^8$ cm^{-3}, however, the central potential well is significantly high enough to push the dust particles away to form a void, shown in Figs. 3(f) and 6(a).

The reason why the potential bump is formed in the central region can be understood as follows. A potential in a cylindrical system can be approximately written as $V=V_0\Sigma A_n(z)J_n(r)$ where $J_n(r)$ is the nth-order Bessel function. From the boundary condition at the center $\partial/\partial r=0$, the contribution from the zeroth-order Bessel function to the potential is then important. Physically, it corresponds to the cylindrical effect, where more streaming ions diverge from the center than in a slab geometry. For example, for a central area with a typical size L and height Δ above the bottom, the streaming area is πL^2 and the horizontal divergence area is $2\pi L\Delta$. Thus the ratio of the out area to the in area is $2\Delta/L$, twice the ratio of Δ/L in the slab geometry.

IV. CONCLUSION

A model with an axisymmetric 3D fluid sheath and MD dust particles has been applied in numerical studies for the formation of dust voids. We found that the formation was due to a potential well in the central region established by the cylindrical electrode with the experimental parameters. The results are in agreement with observed phenomena and data.

ACKNOWLEDGMENTS

This work is supported by the National Natural Science Foundation of China, Grants No. 10175013 and No. 10010760807.

[1] D. Samsonov and J. Goree, Phys. Rev. E **59**, 1047 (1999).
[2] C. O. Thompson, N. D'Angelo, and R. L. Merlino, Phys. Plasmas **6**, 1421 (1999).
[3] G. Prabhuram and J. Goree, Phys. Plasmas **3**, 1212 (1996).
[4] G. E. Morfill, H. M. Thomas, U. Konopka, H. Rothermel, M. Zuzic, A. Ivlev, and J. Goree, Phys. Rev. Lett. **83**, 1598 (1999).
[5] A. Melzer *et al.*, in *Physics of Dusty Plasmas*, edited by M.

Horanyiet *et al.*, AIP Conf. Proc. No. 446 (AIP, Woodbury, NY, 1998), p. 167.
[6] R. P. Dahiya, G. V. Paeva, W. W. Stoffels, E. Stoffels, G. M. W. Kroesen, K. Avinash, and A. Bhattacharjee, Phys. Rev. Lett. **89**, 125001 (2002).
[7] G. V. Paeva *et al.*, in *Dusty Plasmas in the New Millennium* (2002), edited by R. Bharuthram *et al.*, AIP Conf. Proc. No. 649 (AIP, Melville, NY, 2002), p. 188.
[8] X. Wang and A. Bhattacharjee, Phys. Plasmas **7**, 3093 (2000).
[9] J. Goree, G. E. Morfill, V. N. Tsytovich, and S. V. Vladimirov, Phys. Rev. E **59**, 7055 (1999).
[10] V. N. Tsytovich, S. V. Vladimirov, G. E. Morfill, and J. Goree, Phys. Rev. E **63**, 056609 (2001).
[11] K. Avinash, A. Bhattacharjee, and S. Hu, Phys. Rev. Lett. **90**, 075001 (2003).
[12] N. D'Angelo, Phys. Plasmas **5**, 3155 (1998).
[13] A. V. Ivlev *et al.*, Phys. Plasmas **6**, 741 (1999).
[14] K. Avinash, Phys. Plasmas **8**, 351 (2001).
[15] X. Wang, A. Bhattacharjee, S. K. Gou, and J. Goree, Phys. Plasmas **8**, 5018 (2001).
[16] J. H. Chu and L. I. Lin, Phys. Rev. Lett. **72**, 4009 (1994).
[17] Y. Hayashi and K. Tachibana, Jpn. J. Appl. Phys., Part 2 **33**, L804 (1994).
[18] H. Thomas, G. E. Morfill, V. Demmel, J. Goree, B. Feuerbacher, and D. Mohlmann, Phys. Rev. Lett. **73**, 652 (1994).
[19] A. Melzer, T. Trottenberg, and A. Piel, Phys. Lett. A **191**, 301 (1994).
[20] Yu Zhang, Jinyuan Liu, Yue Liu, and X. Wang, Phys. Plasmas **11**, 3840 (2004).
[21] J. Vranjes, M. Y. Tanaka, B. P. Pandey, and M. Kono, Phys. Rev. E **66**, 037401 (2002).
[22] G. B. Arfken and H.-J. Weber, *Mathematical Methods for Physicists*, 5th ed. (Academic Press, San Diego, 2000).
[23] M. D. Kilgore *et al.*, J. Appl. Phys. **73**, 7195 (1993).
[24] M. Lampe *et al.*, Phys. Plasmas **10**, 1500 (2003).
[25] D. S. Lemons, M. S. Murillo, W. Daughton, and Winske, Phys. Plasmas **7**, 2306 (2000).
[26] D. Kremp, M. Schlanges, and W.-D. Kraeft, *Quantum Statistics of Nonideal Plasmas* (Springer-Verlag, Berlin, 2005).
[27] M. Haverlag, G. M. W. Kroesen, T. H. J. Bischops, and F. J. de Hoog, Plasma Chem. Plasma Process. **11**, 357 (1991).
[28] Z. W. Ma and A. Bhattacharjee, Phys. Plasmas **9**, 3349 (2002).